Journal of Cerebral Blood Flow & Metabolism (2010) 30, 323–335
© 2010 ISCBFM All rights reserved 0271-678X/10 $32.00
www.jcbfm.com

Stimulatory effects of thyroid hormone on brain angiogenesis *in vivo* and *in vitro*

Liqun Zhang[1], Christiana Marie Cooper-Kuhn[1], Ulf Nannmark[2], Klas Blomgren[1,3] and Hans Georg Kuhn[1]

[1]*Center for Brain Repair and Rehabilitation, Institute of Neuroscience and Physiology, Sahlgrenska Academy, University of Gothenburg, Göteborg, Sweden;* [2]*Institute of Biomedicine, Sahlgrenska Academy, University of Gothenburg, Göteborg, Sweden;* [3]*Department of Pediatric Oncology, Queen Silvia Children's Hospital, Göteborg, Sweden*

Thyroid hormone is critical for the proper development of the central nervous system. However, the specific role of thyroid hormone on brain angiogenesis remains poorly understood. Treatment of rats from birth to postnatal day 21 (P21) with propylthiouracil (PTU), a reversible blocker of triiodothyronine (T3) synthesis, resulted in decreased brain angiogenesis, as indicated by reduced complexity and density of microvessels. However, when PTU was withdrawn at P22, these parameters were fully recovered by P90. These changes were paralleled by an altered expression of vascular endothelial growth factor A (*Vegfa*) and basic fibroblast growth factor (*Fgf2*). Physiologic concentrations of T3 and thyroxine (T4) stimulated proliferation and tubulogenesis of rat brain-derived endothelial (RBE4) cells *in vitro*. Protein and mRNA levels of VEGF-A and FGF-2 increased after T3 stimulation of RBE4 cells. The thyroid hormone receptor blocker NH-3 abolished T3-induced *Fgf2* and *Vegfa* upregulation, indicating a receptor-mediated effect. Thyroid hormone inhibited the apoptosis in RBE4 cells and altered mRNA levels of apoptosis-related genes, namely *Bcl2* and *Bad*. The present results show that thyroid hormone has a substantial impact on vasculature development in the brain. Pathologically altered vascularization could, therefore, be a contributing factor to the neurologic deficits induced by thyroid hormone deficiency.
Journal of Cerebral Blood Flow & Metabolism (2010) **30,** 323–335; doi:10.1038/jcbfm.2009.216; published online 28 October 2009

Keywords: angiogenesis; apoptosis; endothelial cells; fibroblast growth factor 2; postnatal hypothyroidism; vascular endothelial growth factor

Introduction

Angiogenesis in the brain is a mechanism that is influenced under physiologic and pathologic conditions (Harrigan, 2003; Plate, 1999). New blood vessels are stimulated by the release of proteases from 'active' endothelial cells (ECs), which in turn leads to degradation of the basement membrane, migration of ECs into the interstitial space, EC proliferation, lumen formation, generation of new basement membranes, and recruitment of pericytes. A large number of factors contribute to the promotion of angiogenesis (Folkman, 2003). In the central nervous system (CNS), vascular endothelial growth factor A or B (VEGF-A or VEGF-B) (Namiecinska *et al*, 2005) and platelet-derived growth factor (Cao *et al*, 2008) specifically act on ECs, whereas basic fibroblast growth factor (FGF-2) activates a broad range of target cells, including ECs (Kawamata *et al*, 1997). Thus far, the proangiogenic effect of thyroid hormone has only been studied in peripheral systems. In a thyroid hormone-induced cardiac hypertrophy model, rats displayed substantial coronary angiogenesis that coincided with the upregulated *Fgf2* expression (Tomanek *et al*, 1998). In a chick chorioallantoic membrane model, thyroid hormone exhibited FGF-2-dependent proangiogenic effects (Davis *et al*, 2004). Furthermore, patients who have short-term thyroid hormone deficiency have lower VEGF blood levels that can be reversed by thyroid hormone treatment (Dedecjus *et al*, 2007).

Correspondence: Dr HG Kuhn, Center for Brain Repair and Rehabilitation, Institute for Neuroscience and Physiology, Sahlgrenska Academy at Göteborg University, Medicinaregatan 11, PO Box 432, Göteborg S-40530, Sweden.
E-mail: georg.kuhn@neuro.gu.se
This study was supported by grants from Vetenskapsrådet, The Söderberg Foundation, Hjärnfonden, and LUA/ALF funds for biomedical research.
Received 16 March 2009; revised 11 September 2009; accepted 14 September 2009; published online 28 October 2009

It is well known that the CNS is particularly dependent on the thyroid hormones triiodothyronine (T3) and thyroxine (T4) for normal development and function. The importance of thyroid hormones for proper CNS development is apparent from the severe mental retardation syndrome of cretinism (Smith *et al*, 2002). A lack or excess of thyroid hormone has a marked influence on the structural, biochemical, and functional development of the CNS (Thompson and Potter, 2000). However, the majority of developmental studies have focused on effects on neuronal cells, myelination, and thyroid hormone-regulated genes (Bernal, 2005). In the brain, capillaries consist of particularly densely packed ECs, which specifically prevent entry of many peripheral molecules; however, the role of thyroid hormone on angiogenesis in the CNS remains poorly understood. To our knowledge, this is the first study to address this function.

In this study, propylthiouracil (PTU) was added to the drinking water of postpartum rats to reversibly block thyroid hormone production in nursing rat pups until postnatal day 21 (P21). This developmental stage in rats represents the time period from the third trimester of gestation to the first postnatal years in humans. This study addressed the acute effects of thyroid hormone deficiency on brain vasculature, as well as the long-term recovery effects at postnatal day 90 (P90), a time period in which thyroid hormone levels had returned to normal. Rat brain-derived endothelial (RBE4) cells were cultured with a physiologic concentration of thyroid hormone (10 nmol/L T3 and 100 nmol/L T4, Davis *et al*, 2004; Kansara *et al*, 1996). Angiogenic activity such as EC expansion, migration, tubulogenesis, and apoptosis were investigated. Quantitative real-time PCR (Q-PCR) and enzyme-linked immunosorbent serologic assay (ELISA) were used to measure corresponding mRNA and protein levels involved in the regulation of brain angiogenesis by thyroid hormone.

Materials and methods

Animals

All experiments were conducted in accordance with the university ethics guidelines, and were approved by the Gothenburg committee of the Swedish Agency for Animal Welfare (application no. 421-2004). Pregnant Wistar rats (Charles River, Sulzfeld, Germany) were singly housed in cages until birth, after which litters were culled to eight pups per cage, so that treated mothers could provide sufficient milk for the pups. The animal litters were randomly divided into control and hypothyroid groups. To establish a hypothyroidism rat model, 6-*N*-propyl-2-thiouracil (PTU, Sigma-Aldrich, Stockholm, Sweden) was administered to the drinking water (0.1% w/v). Drinking bottles were replaced daily with fresh PTU solution. Animals underwent PTU treatment from birth until P21, and were subsequently killed. For the long-term survival group, PTU treatment was removed at P22, the pups were weaned at P25 and separated by gender, and were housed in groups of three to four animals until P90.

Plasma Triiodothyronine and Free Thyroxine Assays

Before perfusion, blood was collected directly from the heart and centrifuged at $3{,}000 \times g$ for 20 mins to separate the plasma, which was collected and stored at -20°C. Plasma T3 and free thyroxine (FT4) concentrations were determined in all animals using a radioimmunoassay kit (MP Biomedicals, Orangeburg, NY, USA).

Tissue Collection and Preparation

Rats were deeply anesthetized with sodium pentobarbital and transcardically perfused with 0.9% NaCl, followed by 4% paraformaldehyde per 0.1 mol/L phosphate-buffered saline (PBS), pH 7.4. The brains were removed, postfixed for 3 days in 4% paraformaldehyde per 0.1 mol/L PBS, and transferred to 30% sucrose/PBS. The brains were sagitally cut into 40-μm-thick sections using a sliding microtome, and the sections were stored at 4°C in cryo-protectant solution (25% glycerine/25% ethylene glycol in 0.1 mol/L PBS).

To collect the cortical tissue, rats were deeply anesthetized with sodium pentobarbital, and subsequently killed by decapitation. The brains were rapidly removed and rinsed with chilled PBS, pH 7.4. The entire cortex was collected after the brain was separated at midline. For Q-PCR analysis, the dissected tissue was placed in RNAlater (Qiagen, Solna, Sweden), and stored at 4°C for 24 h. The tissue was then stored at -20°C until total RNA extraction. For ELISA, the dissected tissue was directly stored at -70°C until further use.

For transmission electron microscopy, the dissected cortical tissue was cut into small blocks and immersion fixed in Karnowsky's solution (2% paraformaldehyde, 2.5% glutaraldehyde, and 0.05 Na-azide in 0.05 mol/L Na-cacodylate) overnight, followed by postfixation in 1% OsO_4 and 1% potassium ferrocyanide in 0.1 mol/L Na-cacodylate for 2 h. Tissues were treated with 0.5% uranylacetate *en bloc*, dehydrated, and embedded in Agar 100 resin. The first series of 0.5-μm-thick sections was cut and stained with Richardson's stain and evaluated under a light microscope. This evaluation made it possible to trim the blocks for ultra-thin (50 to 60 nm) sections sufficient for transmission electron microscopy. Electron microscopy sections were examined, after contrast staining with lead citrate and uranylacetate, using a LEO912AB transmission electron microscopy (Zeiss, Oberkochen, Germany) equipped with a Megaview III CCD camera (Olympus Soft Imaging Solutions, Hamburg, Germany).

For microvessel isolation, all procedures were carried out at 4°C, as described previously (Yousif *et al*, 2007). Briefly, freshly dissected cortical tissue, obtained from P21 rats, was homogenized and centrifuged at $1{,}000 \times g$ for 10 mins. The collected pellet was suspended in 17.5% dextran, followed by centrifugation at $4{,}400 \times g$ for 15 mins. The subsequent pellet was suspended in 1% bovine serum albumin, passed through 100- and 20-μm Nylon meshes, resulting in pure microvessel samples.

Immunohistochemistry and Immunofluorescence

Immunostaining was performed according to previously published studies (Zhang *et al*, 2009). The following primary antibodies and final concentrations were used: mouse anti-RECA (1:300, AbD Serotec, Düsseldorf, Germany), rabbit anti-thyroid hormone receptor-α1 (TR-α1), mouse anti-TR-β1 (TR-β1), and goat anti-TR-β2 (TR-β2) (all 1:500, Santa Cruz Biotechnology, Heidelberg, Germany). For immunoperoxidase detection, donkey anti-mouse IgG (1:1,000, Jackson Immuno Research, West Grove, PA, USA) was used. For fluorescence detection, the following secondary antibodies were used: donkey anti-rabbit IgG Alexa-555, donkey anti-mouse IgG Alexa-555, and donkey anti-goat Alexa-555 (all 1:1,000, Jackson Immuno Research).

Stereological Quantification

For *in vivo* microvessel analysis, every twelfth sagittal section containing the cortex and dentate gyrus was analyzed from each animal. The number of microvessels, branching points, and average vessel diameter was quantified in a 50×50-μm counting frame, spaced by a 250×250-μm counting grid, using an unbiased, randomized, stereology system (Stereo Investigator, MicroBrightField, Williston, VT, USA). To calculate vascular density, cortical and dentate gyrus volumes were determined by multiplying the traced areas with section height and serial factor (e.g., 12 for a 1:12 series).

Cell Culture

The immortalized rat brain EC line RBE4 was a kind gift from Dr F Roux, and was cultured as described previously (Roux *et al*, 1994). Briefly, culture plates or flasks were coated with 100 μg/mL type I collagen (Roche Molecular Biochemical, Stockholm, Sweden). The RBE4 cells were maintained in 1:1 (v/v) αMEM/Ham's F12 medium (Invitrogen, Renfrewshire, UK) containing 10% fetal bovine serum (Invitrogen), 30 mg/mL geneticin (Invitrogen), 1 ng/mL FGF-2 (Invitrogen), and penicillin/streptomycin solution (Invitrogen). The RBE4 cells were passaged before confluence, and the medium was replaced every other day. To remove thyroid hormone from the culture medium, charcoal-stripped fetal bovine serum (GENTAUR, Brussels, Belgium) was used in the place of fetal bovine serum. Thyroid hormone treatment was induced by adding physiologic concentrations of T3 (10 nmol/L, Sigma) and T4 (100 nmol/L, Sigma) to the charcoal-stripped RBE4 cell culture medium (Davis *et al*, 2004; Kansara *et al*, 1996). The pan-TR inhibitor NH-3 was a gift from Professor Thomas S Scanlan (Oregon Health and Science University, Portland, OR, USA) and used at 10 μmol/L (Lim *et al*, 2002).

RBE4 Cell Adhesion Assay

The effect of thyroid hormone on cell adhesion was tested using RBE4 cells in 96-well plates (Rigot *et al*, 1998). A collagen-coated plate was blocked with 0.5% bovine serum albumin in PBS. A total of 1×10^5 cells were seeded per well in 250 μL charcoal-stripped RBE4 cell medium mixed with thyroid hormone (T3—10 nmol/L or T4—100 nmol/L). The plate was maintained at 37°C for 2 or 4 h. After gentle washing, adhesion of RBE4 cells was measured using the CyQUANT NF Cell Proliferation Assay kit (Invitrogen), which was based on fluorescent dye binding to determine cellular DNA content of attached cells.

RBE4 Cell Migration Assay

The effect of thyroid hormone on the migratory potential of RBE4 cells was tested using an 8-μm pore size Transwell system (Corning, Corning, NY, USA). The collagen-coated upper chamber was maintained at 37°C overnight before use. The upper chamber was filled with 1×10^5 cells in 100 μL of charcoal-stripped RBE4 cell medium. The lower chamber was filled with 600 μL charcoal-stripped RBE4 cell medium mixed with thyroid hormone (T3—10 nmol/L or T4—100 nmol/L). The transwells were incubated at 37°C for 4 h. Cells in the upper chamber were washed away, and migrating cells were quantified on the bottom side of the membrane. The average number of migrating cells per field was assessed by quantifying 10 random fields under a microscope at $\times 20$ magnification.

RBE4 Cell Tubulogenesis Assay

The effect of thyroid hormone on tubulogenesis was tested by determining the formation of capillary-like tubes in 96-well plates loaded with Matrigel (BD Biosciences, Franklin Lakes, NJ, USA). Matrigel was thawed at 4°C overnight before use. A total of 500 μL of Matrigel was mixed with 8.75×10^4 RBE4 cells in a total volume of 250 μL. A volume of 50 μL aliquots of the Matrigel cell mixture were then added to each well and incubated at 37°C for 30 mins to allow gel formation. This was followed by the addition of 250 μL RBE4 cell medium and incubation at 37°C for 48 h. After washing, the cell medium was replaced with charcoal-stripped RBE4 cell medium mixed with thyroid hormone (T3—10 nmol/L or T4—100 nmol/L), which was replaced every 24 h for 4 days. The tube-like structures inside the wells were fixed with 4% formaldehyde and photographed. The total length of the capillary-like network that formed within the Matrigel was measured using Software ImageJ (available at http://rsb.info.nih.gov; developed by Wayne and Rasband, National Institutes of Health, Bethesda, MD, USA) and the NeuronJ plug-in (available at http://www.imagescience.org/meijering/software/neuronj developed by Eric Meijering, Swiss Federal Institute of Technology, Zürich, Switzerland).

RBE4 Cells Expansion Assay

The effect of thyroid hormone on RBE4 cell expansion was determined using 96-well plates. A total of 5,000 RBE4 cells in a total volume of 250 μL RBE4 medium were added to each well of a collagen-coated plate. The microplate was incubated at 37°C for 4 h to allow for cell adhesion. After gently washing, 250 μL of charcoal-stripped RBE4 medium, mixed with thyroid hormone (T3—10 nmol/L or

T4—100 nmol/L), was added to each well. The medium was replaced every 24 h for 4 days. Cell expansion was determined using the CyQUANT NF Cell Proliferation Assay kit (Invitrogen). From parallel cultures, cell pellets were stored at −80°C for Q-PCR. To study receptor-mediated effects, NH-3 (10 μmol/L) was added to T3-treated wells and concentration on the basis of a previous study (Lim *et al*, 2002). The medium was collected and stored at −80°C for quantification of VEGF-A and FGF-2 protein secretion.

RBE4 Cell Death Assay

The effect of thyroid hormone on RBE4 cell death was determined using 24-well plates. A total of 50,000 RBE4 cells in 1 mL of RBE4 medium was added to each well and incubated at 37°C for 24 h. After washing, the medium was replaced with charcoal-stripped RBE4 medium mixed with thyroid hormone (T3—10 nmol/L or T4—100 nmol/L). The medium was replaced every 24 h for 4 days. Cells were detached using Trypsin (Invitrogen) and incubated in lysis buffer. The cytoplasmic fraction was collected by centrifuging the sample at 20,000 × *g* for 10 mins at 4°C. Fragmented cytoplasmic DNA was quantified using the Cell Death Detection ELISA kit (Roche Applied Science, Mannheim, Germany), which measured the amount of cytoplasmic histone-associated DNA fragments due to apoptosis. An additional portion of detached cells was stored at −80°C for Q-PCR.

Quantification of Vascular Endothelial Growth Factor A and Fibroblast Growth Factor-2 Protein Levels

Vascular endothelial growth factor A and FGF-2 protein concentrations were measured using mouse VEGF-A and human FGF-2 immunoassays (Quantikine, R&D Systems, Minneapolis, MN, USA), which have 98% cross-reactivity to rat VEGF-A and 96% cross-reactivity to rat FGF-2, according to the manufacturer. To obtain tissue lysate, the dissected cortical tissue was homogenized at 4°C in 50 mmol/L Tris-HCl with protease inhibitor (Roche Molecular Biochemical), phosphatase inhibitor (phenylmethylsulfonyl fluoride, Sigma), and Na+ orthovandate (Sigma). In all, 30 μg of total protein was used for the assay. The supernatant was collected after centrifugation at 3,000 × *g* for 10 mins at 4°C. To obtain the cytosol fraction, the supernatant was centrifuged at 15,000 × *g* for 30 mins at 4°C. To determine concentrations of VEGF-A and FGF-2 released *in vitro*, the culture medium was centrifuged at 1,500 × *g* for 10 mins at 4°C to remove particles, and then diluted 10 times with Calibrator Diluent RD57, as recommended by the manufacturer. The relative protein concentration was corrected according to the total number of RBE4 cells in the RBE4 cell expansion assay.

Quantitative Real-Time PCR

To determine relative mRNA levels for the genes of interest, total RNA was extracted using the RNeasy Mini kit (Qiagen). RNase-free DNase (Qiagen) was used to remove genomic DNA contamination from extracted total RNA. RNA concentration and quality were evaluated by spectrophotometry (ND-1000, NanoDrop Technologies, Wilmington, DE, USA). cDNA was synthesized from 2 μg of total RNA at 37°C in a 50-μL reaction mixture with 20 ng/μL random hexamers, 1.6 U/μL RNase inhibitor, and 625 μmol/L dNTP mix (Promega, USA). cDNA was diluted 1:4 before Q-PCR and each sample was duplicated during Q-PCR reaction with QuantiTect SYBR Green PCR kit (Qiagen) by using LightCycler (Roche Diagnostics, Mannheim, Germany). Thermal cycling was initiated at 95°C for 5 mins activation, followed by 40 cycles at 95°C for 10 secs, and at 60°C for 30 secs. The absolute expression copy was calculated using the standard curve method and glyceraldehyde-3-phosphate dehydrogenase (*Gapdh*) was used as a reference gene to calculate the relative mRNA concentration. Data are presented as fold change between control and treated groups. The following QuantiTect primers (Qiagen) were used: *Vegfa* (QT00198954), *Fgf2* (QT00189035), *Bax* (QT01081752), *Bad* (QT00190407), *Aifm1* (apoptosis-inducing factor, QT00180943), *Bcl2* (QT00184863), *Bclx1* (QT01081346), *Gapdh* (QT00199633), *Flt1* (vascular endothelial growth factor receptor-1) (QT00183498), and *Flk1* (vascular endothelial growth factor receptor-2) (QT00408352).

Real-Time-PCR of Thyroid Hormone Receptors

Total RNA was generated from isolated microvessels from the cortex or RBE4 cells using the RNeasy Mini kit (Qiagen). Primer pairs for TRs were designed using Primer3 software (http://frodo.wi.mit.edu/; Massachusetts Institute of Technology, Cambridge, MA, USA). Basic Local Alignment Search Tool (BLAST) was used to ensure specificity of the primer pair. The primer pairs were as follows: thyroid hormone receptor alpha 1 (*Thra1*) forward 5′-ccc cca tct ctt ctc tcc tt-3′ and reverse 5′-aag ttc att tgt cgc cct gt-3′; thyroid hormone receptor beta 1 (Thrb1) forward 5′-tcg ctg tag act tgg tgt gg-3′ and reverse 5′-ctc ttt gga cgg aga act gg-3′; and thyroid hormone receptor beta 2 (Thrb2) 5′-ggt ggt tat tca tcc cct ctc-3′ and reverse 5′-tgg cac gca gta gtt cat tt-3′. Real-time-PCR products were separated by electrophoresis on a 1% agarose gel and visualized using SYBR Green.

Statistical Analysis

Statistical analysis was carried out using equal variances of two-sample *t*-test to compare differences between control and PTU-treated animals or thyroid hormone-treated cells. For comparison of three *in vitro* groups (Control, TH, TH + NH-3), analysis of variance (ANOVA) for matched observation was used in conjunction with Tukey's *post hoc* test. All cell assays were independently repeated at least thrice. Error bars represent s.e.m.; significance difference was assumed at the 5% level and indicated as $P < 0.05$.

Results

Postnatal Propylthiouracil Exposure Reduced Thyroid Hormone Levels

The thyroid hormone status was determined by measuring FT4 and T3 plasma concentrations and

presented in a previous study (Zhang *et al*, 2009). In brief, postnatal exposure to PTU significantly decreased FT4 (28-fold) and T3 (5.6-fold) concentrations at P21; however, on discontinuing PTU treatment at P22, thyroid hormone levels (FT4 and T3) returned to control levels by P90.

Postnatal Thyroid Hormone Deficiency Decreased Central Nervous System Angiogenesis

The effects of postnatal hypothyroidism on brain microvasculature were analyzed in the rat cortex and dentate gyrus at P21, the final day of PTU treatment, and 2.5 months later (P90), a time point at which thyroid hormone levels had returned to normal. At the end of PTU treatment (P21), vascular distribution was reduced, but larger microvessels were present in the cortex (Figures 1A–1D) and dentate gyrus (Figures 2A–2D). At P21, microvessel complexity, as measured by quantifying the number of branching points, was significantly decreased by PTU treatment in the cortex and dentate gyrus (Figure 1E, $P<0.002$ and Figure 2E, $P<0.002$, respectively). Similarly, microvessel density was decreased in both regions (Figure 1F, $P<0.005$ and

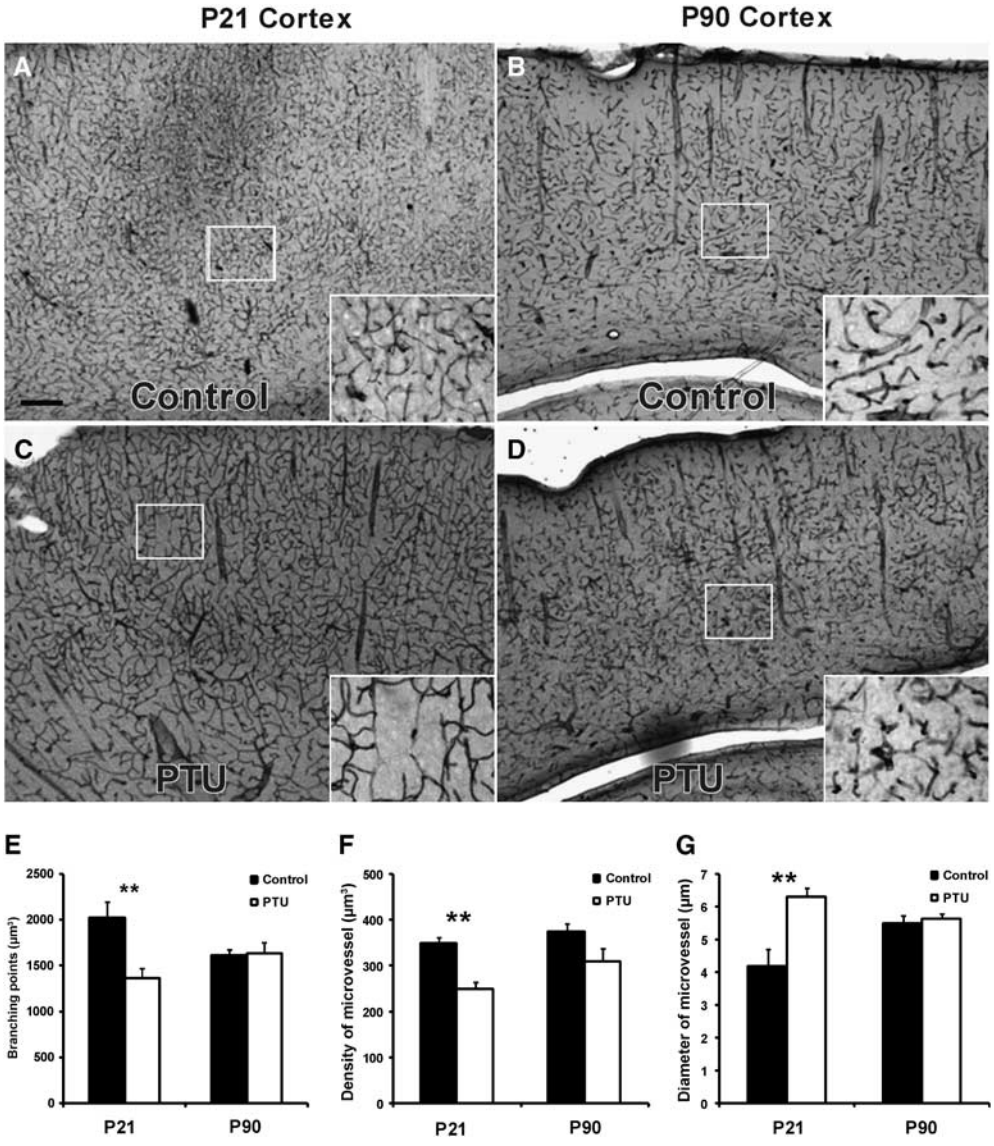

Figure 1 Effects of postnatal thyroid hormone deficiency on microvessels in the neocortex. Postnatal hypothyroidism was induced with PTU in the drinking water from birth to P21. Immunohistochemistry staining of mouse anti-RECA (microvessel marker) showed visible changes in the cortical microvessels at P21 in the PTU-treated rats (**A** and **B**), with full recovery by P90 (**C** and **D**). Quantitative analysis of cortical microvessels was based on several parameters: branching point (**E**), microvessel density (**F**), and microvessel diameter (**G**) in 40-μm-thick, sagittal sections. At P21, PTU treatment resulted in decreased branching points, decreased microvessel density, and enlarged microvessel diameter. However, by P90, these changes were no longer apparent. Data are presented as mean ± s.e.m. from P21 ($n = 8$) and P90 rats ($n = 16$, 8 male and 8 female). Two-sample equal variance *t*-test was applied, $^{**}P < 0.01$. Scale bar in panel A = 50 μm.

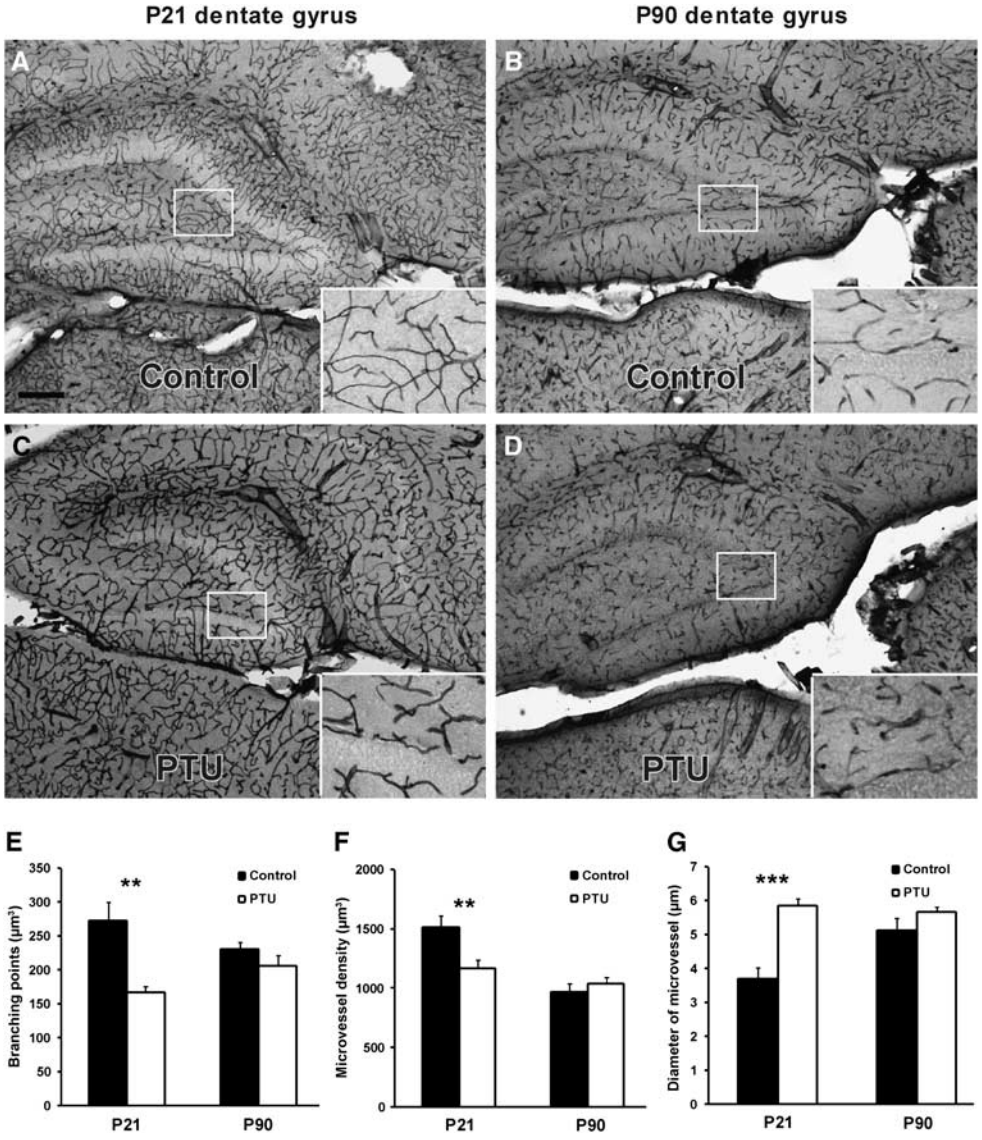

Figure 2 Effects of postnatal thyroid hormone deficiency on microvessels in the dentate gyrus. Postnatal hypothyroidism was induced with PTU in the drinking water from birth to P21. Immunohistochemistry staining of mouse anti-RECA (microvessel marker) showed visible changes of microvessels in the dentate gyrus at P21 in the PTU-treated rats (**A** and **B**), with full recovery at P90 (**C** and **D**). Quantitative analysis of dentate gyrus microvessels was based on several parameters: branching points (**E**), microvessel density (**F**), and microvessel diameter (**G**) in 40-μm-thick, sagittal sections. At P21, PTU treatment resulted in decreased branching points, decreased microvessel density, and enlarged diameter of microvessel. However, by P90, these changes were no longer apparent. Data are presented as mean ± s.e.m. from P21 ($n = 8$) and P90 rats ($n = 16$, 8 male and 8 female). Two-sample equal variance *t*-test was applied, $***P < 0.001$, $**P < 0.01$. Scale bar in panel A = 50 μm.

Figure 2F, $P < 0.01$, respectively). However, in both regions, microvessel diameter was significantly increased (Figure 1G, $P < 0.002$ and Figure 2G, $P < 0.001$, respectively) by thyroid hormone deficiency. At P90 in the PTU-treated rats, these parameters had returned control levels in the cortex and dentate gyrus (Figures 1E–1G and Figures 2E–2G, respectively).

At the ultrastructural level, we observed no changes in the P21 PTU-treated cortex in the composition with the microvessels, with regard to EC or pericyte morphology, basal membrane configuration or thickness (Figure 3), nor did the astrocyte endfeet morphology differ between the groups (data not shown).

Reduced Levels of Fibroblast Growth Factor-2 and Vascular Endothelial Growth Factor A During Postnatal Thyroid Hormone Deficiency

To identify angiogenic changes due to thyroid hormone deficiency at transcriptional and protein levels, relatively levels of two prominent proangiogenic factors, FGF-2 and VEGF-A, were measured at P21 and P90 in the cortex using Q-PCR and ELISA

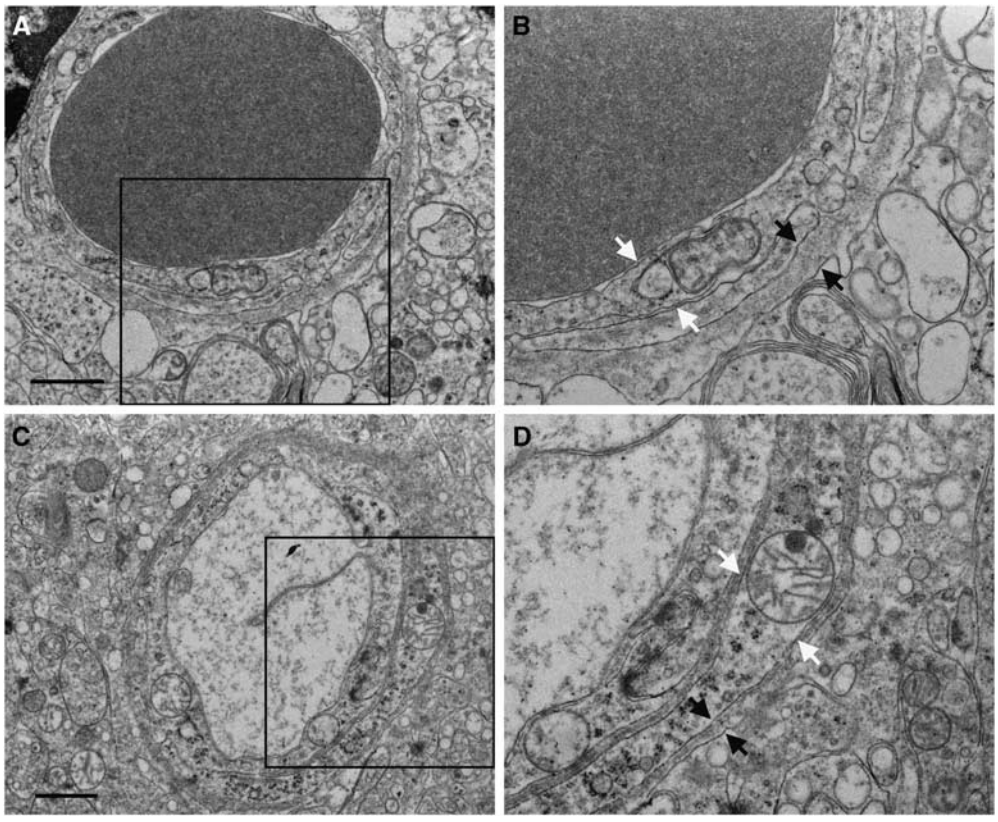

Figure 3 Electron microscopy of cortical microvessels at postnatal day 21. Microvessels from PTU-treated animals (**A** and **B**) and control animals (**C** and **D**) appear to have normal endothelial cell (white arrows) and basal membrane structure (black arrows). Panels B and D are enlargements of the framed areas in panels A and C, respectively. Scale bar in panels A and C = 1 μm.

analyses, respectively. At P21 in PTU-treated rats (Figure 4A), mRNA levels of *Fgf2* ($P<0.02$), *Vegfa* ($P<0.001$), and *Flk1* (VEGFR-2) ($P<0.001$) were significantly decreased. However, PTU treatment did not alter *Flt1* (VEGFR-1) mRNA levels ($P=0.345$). At P90, when thyroid hormone levels had returned to normal, mRNA levels of *Fgf2*, *Vegfa*, and *Flk1* (VEGFR-2) also reached control levels. However, *Flt1* (VEGFR-1) mRNA levels remained decreased at P90 ($P<0.01$) (Figure 4B). At the protein level, PTU treatment significantly decreased the production of FGF-2 and VEGF-A protein in the cortex at P21 (Figure 4C, both $P<0.04$). However, this reduction had recovered by P90 (Figure 4D).

Brain Endothelial Cells Express Thyroid Hormone Receptors *In Vivo* and *In Vitro*

Total RNA was extracted from the isolated microvessels cortex of P21 rats (Figure 5A). All three thyroid hormone receptors (*Thra1*, *Thrb1*, *Thrb2*) were expressed in the CNS microvasculature, as detected by RT-PCR (Figure 5B). Total RNA was extracted from RBE4 cells, and analysis confirmed that all three receptors were also expressed in brain ECs *in vitro* (Figure 5D). Immunofluorescence staining showed colocalization of RECA (EC marker) and TR-β1 (Figure 5C). Similar results were obtained for TR-α1 and TR-β2 (data not shown).

Thyroid Hormone Stimulated Central Nervous System Angiogenesis *In Vitro*

The effect of thyroid hormone on, *in vitro*, microvessel generation was investigated using thyroid hormone at the physiologic level (normal serum concentration: T3 = 10 nmol/L and T4 = 100 nmol/L). Distinct processes of microvessel generation were analyzed using RBE4 cells, such as cell expansion, adhesion, migration, capillary tube formation, and apoptosis. After RBE4 cells were incubated on collagen-coated microplates for 4 h, neither T3 (10 nmol/L) nor T4 (100 nmol/L) exerted any effect on cell adhesion potential, when compared with untreated cells (Figure 6A, T3: $P=0.58$, T4: $P=0.20$). The Transwell system was then used to assess the migration effects of thyroid hormone. After incubation with thyroid hormone for 4 h, there was no change in the number of RBE4 cells that migrated toward the thyroid hormone source, compared with nontreated wells (Figure 6B, T3: $P=0.12$, T4: $P=0.47$).

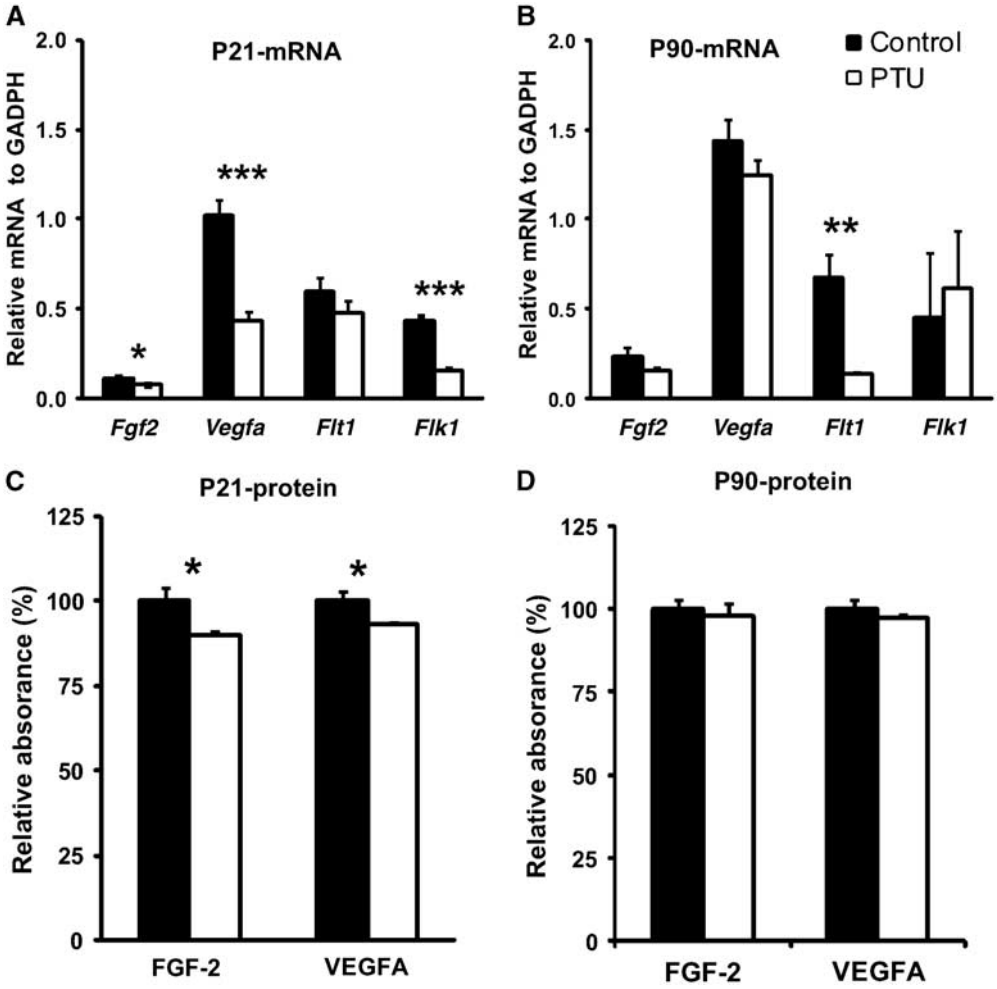

Figure 4 *In vivo* analysis of relative levels of FGF-2 (basic fibroblast growth factor) and VEGF-A (vascular endothelial growth factor A) in the cortex. Tissue was collected during PTU treatment (P21) and after PTU treatment (P90). The relative mRNA levels of *Fgf2*, *Vegfa* and *Flk1* (VEGFR-2) were reduced at P21 (**A**), but recovered to normal levels by P90 (**B**), as measured by Q-PCR. *Flt1* (VEGFR-1) mRNA levels remained unchanged at P21, but decreased by P90 (panels A and B). The relative amount of protein expression of FGF-2 and VEGF-A were reduced at P21 (panel C), but recovered to normal levels by P90 (panel D). Data represent mean ± s.e.m. from P21 ($n = 4$) and P90 rats ($n = 6$, 3 male and 3 female). Two-sample equal variances *t*-test was applied, $***P < 0.001$, $**P < 0.01$, $*P < 0.05$.

After 4 days of thyroid hormone treatment, cell expansion was measured by fluorescent dye incorporation into DNA. Increased fluorescent dye incorporation was observed after treatment with 10 nmol/L T3 (155%, $P < 0.001$) and 100 nmol/L T4 (122%, $P < 0.01$) (Figure 6C). To further investigate the effects of thyroid hormone on cell expansion, cell death was measured in RBE4 cells using a DNA fragmentation assay. Up to 30% reduced cell death was observed after incubation with T3 and 20% with T4 (Figure 6D). In addition, using Matrigel-embedded RBE4 cells, the effect of thyroid hormone on endothelial tube formation was observed. After 4 days of thyroid hormone treatment, the length of tube-like structures significantly increased by T3 (234%, $P < 0.001$) and T4 (163%, $P < 0.01$), compared with nontreated wells (Figures 6E and 6F).

Thyroid Hormone Influenced Fibroblast Growth Factor-2 and Vascular Endothelial Growth Factor A Expression *In Vitro*

The effects of thyroid hormone on transcriptional and protein levels of VEGF-A and FGF-2, as well as their receptors, were measured used Q-PCR and ELISA. After 4 days of treatment, T3 (10 nmol/L) significantly increased *Vegfa* mRNA expression (Figure 7A, $P < 0.01$); however, *Fgf2* expression remained unchanged. Vascular endothelial growth factor receptor-2 expression remained unchanged by T3 (10 nmol/L), but was reduced by T4 (100 nmol/L). Vascular endothelial growth factor-R1 mRNA levels were unaffected by either treatment. At the protein level, T3 (10 nmol/L) significantly increased FGF-2 expression by 16% (Figure 7B, $P < 0.01$) and VEGF-A by 22%, as determined by ELISA (Figure 7C,

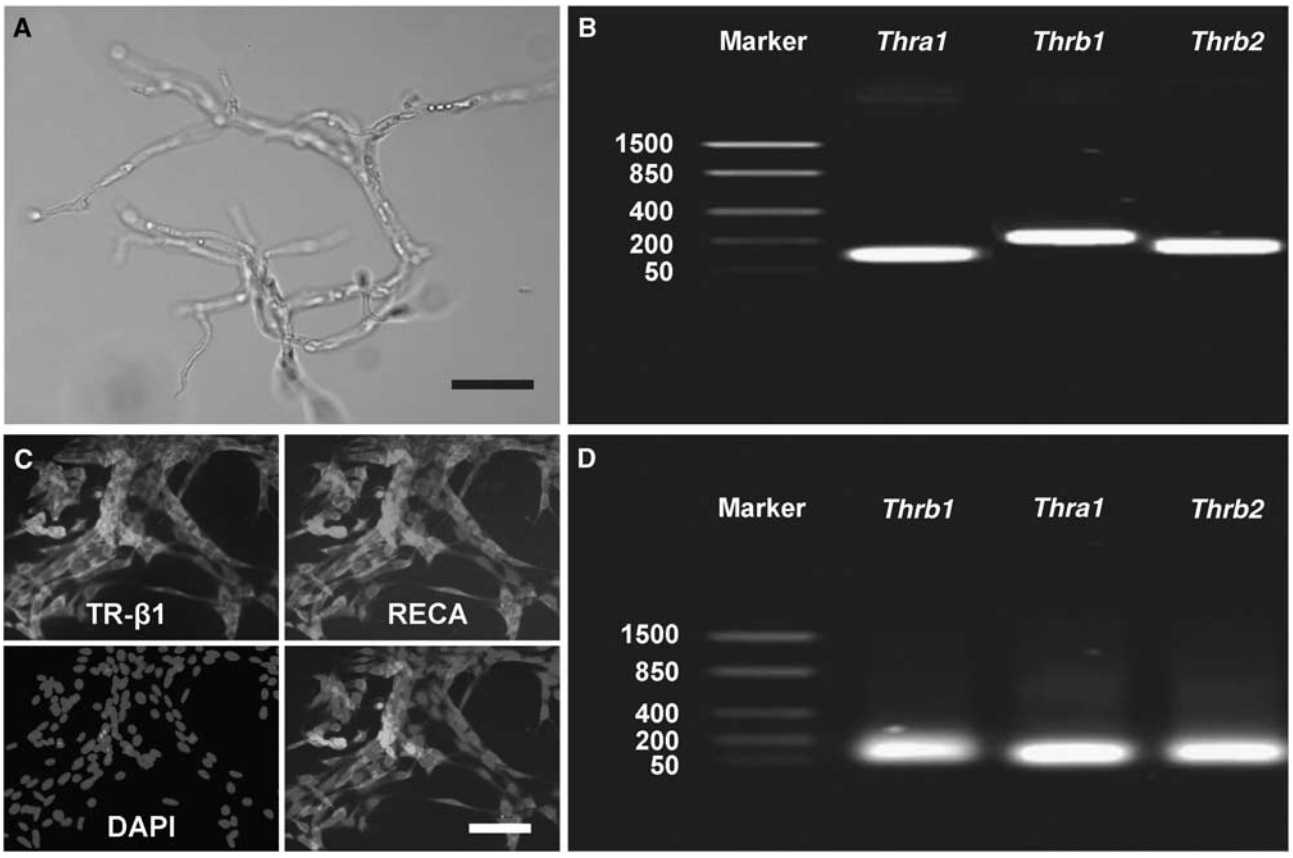

Figure 5 Thyroid hormone receptor (TR) expression in microvessels of the cortex and REB4 cells. (**A**) Purely isolated microvessels from the rat cortex. (**B**) TR expression in isolated microvessels determined by RT-PCR. (**C**) Immunohistochemistry staining of RBE4 cells against TR-β1 (orange signal) and RECA (green signal) revealed intense expression by endothelial cells (DAPI nuclear staining in blue). Immunostaining against TR-α1 and TR-β2 obtained similar results (data not shown). (**D**) TR expression in RBE4 cells determined by RT-PCR. Scale bar in panel A = 250 μm and in panel C = 25 μm.

$P<0.001$). However, T4 (100 nmol/L) had no effect on the expression of these growth factors. To determine whether the change in protein expression is mediated through TRs, we used the pan-TR blocker NH-3. The T3-mediated increase in VEGF and FGF-2 protein was blocked by NH-3, as protein levels were significantly reduced (Figures 7D and 7E, $P<0.01$).

Thyroid Hormone Influenced the Expression of Apoptosis-Related Genes

The relative transcriptional level of genes involved in the regulation of programmed cell death (Figure 7F) was measured. Cells treated with T3 (10 nmol/L) exhibited decreased mRNA levels of the proapoptotic gene, *Bad*, and increased levels of the anti-apoptotic gene *Bcl2*. The proapoptotic genes, AIF and Bax, were unaffected by T3 treatment. Expression of these genes remained unaffected after treatment with T4 (100 nmol/L).

Discussion

Thyroid hormone exerts dynamic effects on the vasculature during CNS development. Transiently induced postnatal hypothyroidism results in a significantly reduced angiogenesis in the brain. However, with recovery of thyroid hormone levels toward adulthood, the vascular system is observed to recover. These cellular changes are paralleled by altered expression of angiogenic factors, such as VEGF-A and FGF-2. In addition, this study showed that, for RBE4 cells, thyroid hormone acts as a specific stimulator of tubulogenesis *in vitro*, as well as an inhibitor of cell apoptosis. Results showed that autocrine regulation from VEGF-A and FGF-2 could contribute to thyroid hormone effects on brain ECs.

The present *in vivo* data are the first to show reduced angiogenesis in the rat brain after postnatal hypothyroidism. This deficiency was observed as reduced complexity and density, as well as increased microvessel diameter within the cortex and dentate gyrus. These changes were considered to be a result of pathologic changes due to thyroid hormone deficiency, rather than because of developmental retardation of the vascular system, because no significant changes during normal rat development (P1–21) in capillary density or diameter have been reported previously (Michaloudi *et al*, 2006). The results of our study that shows reduced vascular

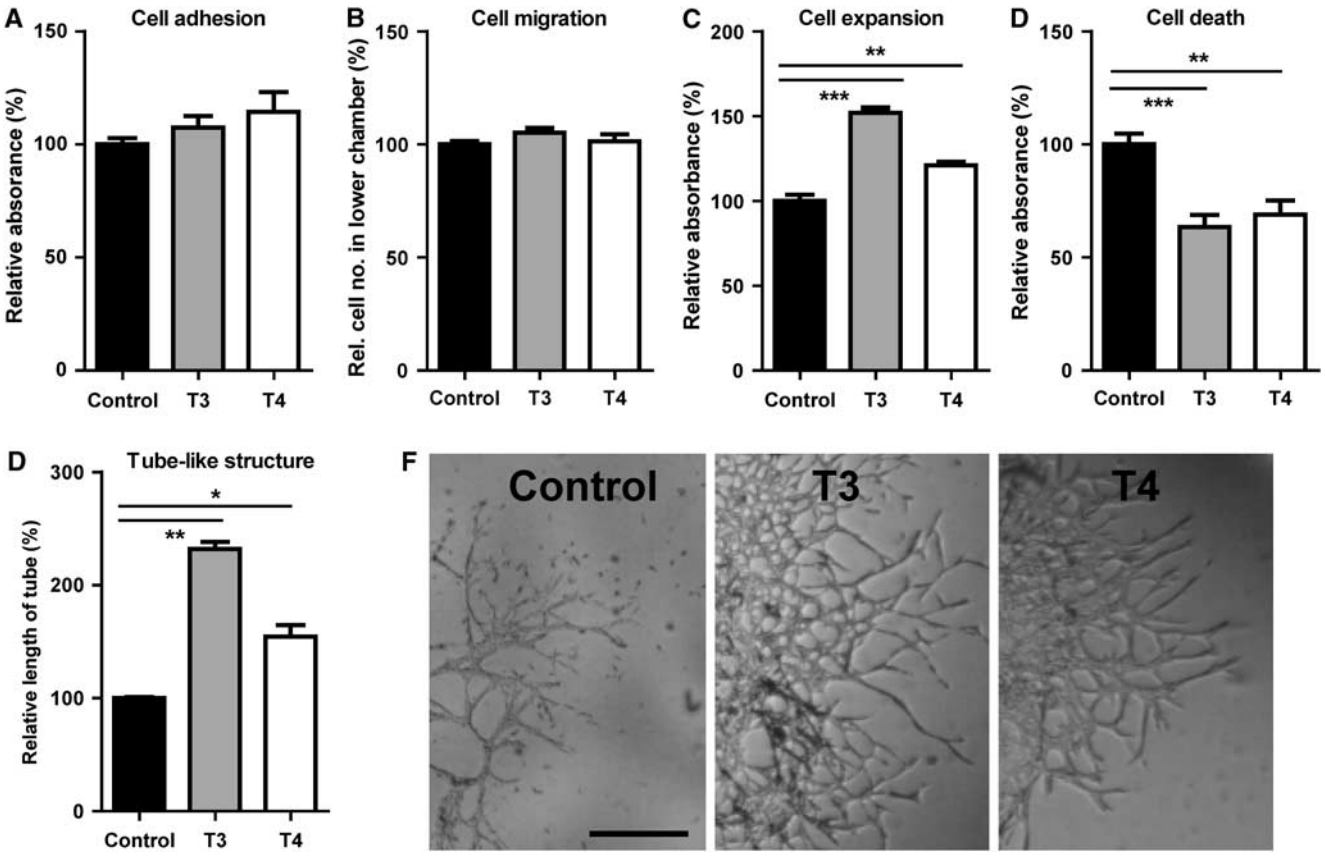

Figure 6 Effects of thyroid hormone on REB4 cell adhesion, migration, expansion, apoptosis, and tube-like structure formation *in vitro*. Both T3 (10 nmol/L) and T4 (100 nmol/L) had no effect on the ability of RBE4 cells to adhere (**A**) or migrate (**B**). However, T3 and T4 increased expansion of RBE4 cells (**C**), decreased apoptosis (**D**), and increased tube-like structure formation (**E**). Representative images of tube-like structures are depicted in (**F**). All cell assay results were expressed as percentage of control and were repeated three independent times. Two-sample equal variances *t*-test was applied, $***P < 0.001$, $**P < 0.01$, $*P < 0.05$. Scale bar in panel F = 15 μm.

complexity and density might explain previous results of dramatically decreased cerebral blood flow in PTU-treated rats (Lefauconnier *et al*, 1985) and changes in the blood–brain barrier nutrient transport in iodine-deficient animals (Sunitha *et al*, 1997). However, hypothyroid-induced changes in the brain capillaries are not necessarily in line with peripheral angiogenesis studies, in which increased myocardial capillary proliferation was induced by PTU-treatment (Heron and Rakusan, 1994). These angiogenic changes due to thyroid hormone deficiency are likely to cause a substantial imbalance of nutrient and trophic factor support from the blood stream, which could further impair postnatal brain development and function.

In the adult, after PTU withdrawal at P22, the brain vasculature appeared to fully recover, as determined by capillary complexity, density, and diameter. Vascular endothelial growth factor-A and FGF-2 also returned to normal levels, which indicated recovery at molecular and cellular levels. Hypothyroidism did not result in any ultrastructural changes to the brain capillaries, which could also contribute to full recovery of the vascular system in the adult brain. These findings are in line with other studies, indicating full or partial recovery of physiologic parameters after reversal of developmental thyroid hormone deficiency, such as hippocampal volume changes and cytochrome oxidase levels (Farahvar and Meisami, 2007), as well as hippocampal cholinergic activity (Sawin *et al*, 1998) and proliferation of olfactory receptor neurons (Paternostro and Meisami, 1996).

This study provides, for the first time, strong evidence that thyroid hormone exhibits direct proangiogenic effects on brain ECs. Results showed that T3 and T4 increased brain EC expansion and formation of tube-like structures. The current experiments used a single doses of T3 (10 nmol/L) and T4 (100 nmol/L) in the range of physiologic levels, which have previously been shown to be effective *in vitro* (Kansara *et al*, 1996). However, we cannot exclude the fact that higher levels may have different effects in our system. In human foreskin ECs, T3 exhibited no effects on tubulogenesis although applied at 1 μmol/L, a 100 $\times$ fold higher concentration (Lansink *et al*, 1998). A lower concentration of T3 (1 nmol/L) reduced cell adhesion and stimulated

migration in human mesenchymal stem cells (Benvenuti *et al*, 2008).

Thyroid hormone exerts its cellular effects through its receptors largely through genomic targets, and also through nongenomic mechanisms (Bassett *et al*, 2003; Lakatos and Stern, 1991). Expression of TRs in the brain has been characterized (Bernal, 2005; Bradley, 1992, Forrest *et al*, 1990; Porterfield and Hendrich, 1993). Thyroid hormone receptor-α1 predominates throughout prenatal brain development, with highest levels being found in the hippocampus, cerebral cortex, piriform cortex, and superior colliculus. However, TR-β1 and TR-β2 are mainly expressed postnatally. We observed the expression of all three receptors in ECs isolated from the postnatal brain and the pan-TR blocker; NH-3 was able to block the effect of T3 on ECs *in vitro*. Future experiments would be required to show the relative contribution of the different receptors to the observed effect.

Our data show reduced apoptosis of ECs by T3 and T4 treatment. At the molecular level, we observed reduced expression of the proapoptotic gene *Bad* and increased expression of the antiapoptotic gene *Bcl2 in vitro*. This was in accordance with reduced *Bcl2* expression in other CNS cell types due to hypothyroidism, such as cerebellar neurons (Muller *et al*, 1995; Singh *et al*, 2003), and shows the importance of thyroid hormone for cell survival in the brain.

Most frequently, thyroid hormone deficiency has been associated with neurogenesis defects (Ambrogini *et al*, 2005; Desouza *et al*, 2005; Zhang *et al*, 2000) and decreased myelination (Ibarrola and Rodriguez-Pena, 1997). Nevertheless, the effect of angiogenesis as a contributing factor in these defects remains poorly understand. In songbirds, it has been shown that hormone-induced angiogenesis is required for increased neurogenesis during song learning (Louissaint *et al*, 2002). Testosterone-induced VEGF production leads to angiogenesis and release of brain-derived neurotrophic factor from ECs, which in turn stimulates adult neurogenesis in the higher vocal center. Altogether, the present results and previous studies raise the interesting hypothesis that decreased angiogenesis not only leads to reduced levels of nutrients but also directly affects the level of neurotrophic proteins. This could further impair neuronal development and contribute to cognitive retardation observed in postnatal hypothyroidism. With regard to treatment of postnatal hypothyroidism, early restoration of angiogenic mechanisms could be a therapeutic target for functional recovery.

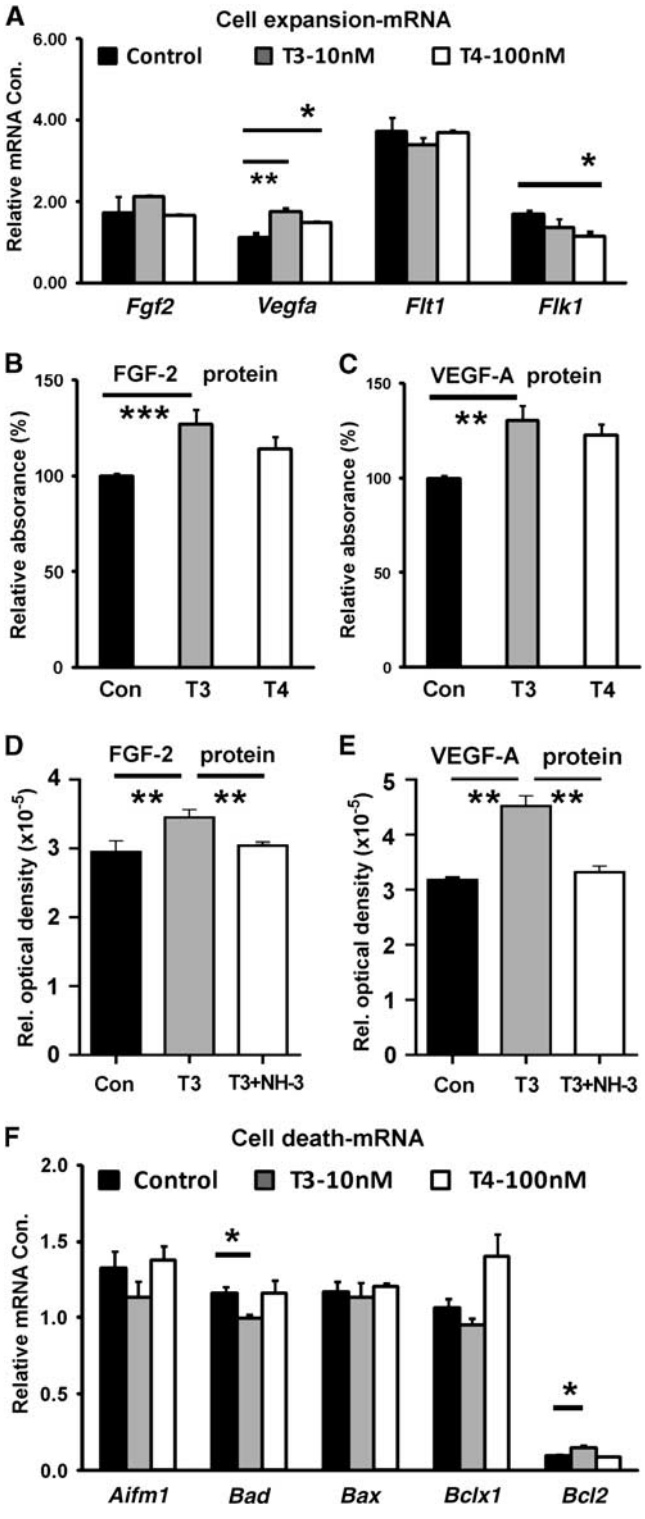

Figure 7 Expression of FGF-2 and VEGF-A, as well as apoptosis-related genes, during *in vitro* cell expansion. T3 (10 nmol/L) and T4 (100 nmol/L) increased the relative levels of *Vegfa* mRNA expression, but T3 decreased *Flk1* (VEGFR-2) mRNA expression (**A**). T3 treatment increased the relative amounts of FGF-2 (**B**) and VEGF-A (**C**) protein expression, but T4 had no effect. (**D** and **E**) Protein levels of FGF-2 and VEGF-A were normalized by adding thyroid hormone receptor blocker NH-3. (**F**) T3 treatment increased mRNA expression of the antiapoptotic gene *Bcl2*, but reduced mRNA expression of the proapoptotic gene *Bad*. Cell assay results were expressed as percentage of control and were repeated three independent times. Two-sample equal variances *t*-test was used in panels A, B, C and F and ANOVA in panels D and E, $***P < 0.001$, $**P < 0.01$, $*P < 0.05$.

Overall, the present findings showed that the detrimental effects of thyroid hormone deficiency in the developing brain might be related to angiogenesis and subsequent insufficient trophic support, as well as to the direct effects on neurons or glial cells. These data contribute to the understanding of the effects of thyroid hormone on angiogenic mechanisms in normal and hypothyroid conditions. This study could have important implications for the therapeutic targeting of angiogenesis in thyroid hormone-related mental retardation.

Conflict of interest

The authors declare no conflict of interest.

Acknowledgements

The authors thank Prof Thomas S Scanlan for providing the thyroid hormone receptor antagonist NH-3 and Dr F Roux for providing the RBE4 cells.

References

Ambrogini P, Cuppini R, Ferri P, Mancini C, Ciaroni S, Voci A, Gerdoni E, Gallo G (2005) Thyroid hormones affect neurogenesis in the dentate gyrus of adult rat. *Neuroendocrinology* 81:244–53

Bassett JH, Harvey CB, Williams GR (2003) Mechanisms of thyroid hormone receptor-specific nuclear and extra nuclear actions. *Mol Cell Endocrinol* 213:1–11

Benvenuti S, Luciani P, Cellai I, Deledda C, Baglioni S, Saccardi R, Urbani S, Francini F, Squecco R, Giuliani C, Vannelli GB, Serio M, Pinchera A, Peri A (2008) Thyroid hormones promote cell differentiation and up-regulate the expression of the seladin-1 gene in in vitro models of human neuronal precursors. *J Endocrinol* 197:437–46

Bernal J (2005) Thyroid hormones and brain development. *Vitam Horm* 71:95–122

Bradley DJ, Towle HC, Young WS 3rd (1992) Spatial and temporal expression of alpha- and beta-thyroid hormone receptor mRNAs, including the beta 2-subtype, in the developing mammalian nervous system. *J Neurosci* 12:2288–302

Cao Y, Cao R, Hedlund EM (2008) R Regulation of tumor angiogenesis and metastasis by FGF and PDGF signaling pathways. *J Mol Med* 86:785–9

Davis FB, Mousa SA, O'Connor L, Mohamed S, Lin HY, Cao HJ, Davis PJ (2004) Proangiogenic action of thyroid hormone is fibroblast growth factor-dependent and is initiated at the cell surface. *Circ Res* 94:1500–6

Dedecjus M, Kolomecki K, Brzezinski J, Adamczewski Z, Tazbir J, Lewinski A (2007) Influence of L-thyroxine administration on poor-platelet plasma VEGF concentrations in patients with induced short-term hypothyroidism, monitored for thyroid carcinoma. *Endocr J* 54:63–9

Desouza LA, Ladiwala U, Daniel SM, Agashe S, Vaidya RA, Vaidya VA (2005) Thyroid hormone regulates hippocampal neurogenesis in the adult rat brain. *Mol Cell Neurosci* 29:414–26

Farahvar A, Meisami E (2007) Novel two-dimensional morphometric maps and quantitative analysis reveal marked growth and structural recovery of the rat hippocampal regions from early hypothyroid retardation. *Exp Neurol* 204:541–55

Folkman J (2003) Fundamental concepts of the angiogenic process. *Curr Mol Med* 3:643–51

Forrest D, Sjoberg M, Vennstrom B (1990) Contrasting developmental and tissue-specific expression of alpha and beta thyroid hormone receptor genes. *EMBO J* 9:1519–28

Harrigan MR (2003) Angiogenic factors in the central nervous system. *Neurosurgery* 53:639–60; discussion 60–61

Heron MI, Rakusan K (1994) Geometry of coronary capillaries in hyperthyroid and hypothyroid rat heart. *Am J Physiol* 267:H1024–31

Ibarrola N, Rodriguez-Pena A (1997) Hypothyroidism coordinately and transiently affects myelin protein gene expression in most rat brain regions during postnatal development. *Brain Res* 752:285–93

Kansara MS, Mehra AK, Von Hagen J, Kabotyansky E, Smith PJ (1996) Physiological concentrations of insulin and T3 stimulate 3T3-L1 adipocyte acyl-CoA synthetase gene transcription. *Am J Physiol* 270:E873–81

Kawamata T, Speliotes EK, Finklestein SP (1997) The role of polypeptide growth factors in recovery from stroke. *Adv Neurol* 73:377–82

Lakatos P, Stern PH (1991) Evidence for direct nongenomic effects of triiodothyronine on bone rudiments in rats: stimulation of the inositol phosphate second messenger system. *Acta Endocrinol (Copenh)* 125:603–8

Lansink M, Koolwijk P, van Hinsbergh V, Kooistra T (1998) Effect of steroid hormones and retinoids on the formation of capillary-like tubular structures of human microvascular endothelial cells in fibrin matrices is related to urokinase expression. *Blood* 92:927–38

Lefauconnier JM, Lacombe P, Bernard G (1985) Cerebral blood flow and blood-brain influx of some neutral amino acids in control and hypothyroid 16-day-old rats. *J Cereb Blood Flow Metab* 5:318–26

Lim W, Nguyen NH, Yang HY, Scanlan TS, Furlow JD (2002) A thyroid hormone antagonist that inhibits thyroid hormone action in vivo. *J Biol Chem* 277: 35664–70

Louissaint A Jr, Rao S, Leventhal C, Goldman SA (2002) Coordinated interaction of neurogenesis and angiogenesis in the adult songbird brain. *Neuron* 34:945–60

Michaloudi H, Batzios C, Grivas I, Chiotelli M, Papadopoulos GC (2006) Developmental changes in the vascular network of the rat visual areas 17, 18 and 18a. *Brain Res* 1103:1–12

Muller Y, Rocchi E, Lazaro JB, Clos J (1995) Thyroid hormone promotes BCL-2 expression and prevents apoptosis of early differentiating cerebellar granule neurons. *Int J Dev Neurosci* 13:871–85

Namiecinska M, Marciniak K, Nowak JZ (2005) VEGF as an angiogenic, neurotrophic, and neuroprotective factor. *Postepy Hig Med Dosw (Online)* 59:573–83

Paternostro MA, Meisami E (1996) Essential role of thyroid hormones in maturation of olfactory receptor neurons: an immunocytochemical study of number and cytoarchitecture of OMP-positive cells in developing rats. *Int J Dev Neurosci* 14:867–80

Plate KH (1999) Mechanisms of angiogenesis in the brain. *J Neuropathol Exp Neurol* 58:313–20

Porterfield SP, Hendrich CE (1993) The role of thyroid hormones in prenatal and neonatal neurological development–current perspectives. *Endocr Rev* 14:94–106

Rigot V, Lehmann M, Andre F, Daemi N, Marvaldi J, Luis J (1998) Integrin ligation and PKC activation are required for migration of colon carcinoma cells. *J Cell Sci* 111 (Pt 20):3119–27

Roux F, Durieu-Trautmann O, Chaverot N, Claire M, Mailly P, Bourre JM, Strosberg AD, Couraud PO (1994) Regulation of gamma-glutamyl transpeptidase and alkaline phosphatase activities in immortalized rat brain microvessel endothelial cells. *J Cell Physiol* 159: 101–13

Sawin S, Brodish P, Carter CS, Stanton ME, Lau C (1998) Development of cholinergic neurons in rat brain regions: dose-dependent effects of propylthiouracil-induced hypothyroidism. *Neurotoxicol Teratol* 20:627–35

Singh R, Upadhyay G, Kumar S, Kapoor A, Kumar A, Tiwari M, Godbole MM (2003) Hypothyroidism alters the expression of Bcl-2 family genes to induce enhanced apoptosis in the developing cerebellum. *J Endocrinol* 176:39–46

Smith JW, Evans AT, Costall B, Smythe JW (2002) Thyroid hormones, brain function and cognition: a brief review. *Neurosci Biobehav Rev* 26:45–60

Sunitha Y, Udaykumar P, Raghunath M (1997) Changes in blood-brain barrier nutrient transport in the offspring of iodine-deficient rats and their preventability. *Neurochem Res* 22:785–90

Thompson CC, Potter GB (2000) Thyroid hormone action in neural development. *Cereb Cortex* 10:939–45

Tomanek RJ, Doty MK, Sandra A (1998) Early coronary angiogenesis in response to thyroxine: growth characteristics and upregulation of basic fibroblast growth factor. *Circ Res* 82:587–93

Yousif S, Marie-Claire C, Roux F, Scherrmann JM, Decleves X (2007) Expression of drug transporters at the blood-brain barrier using an optimized isolated rat brain microvessel strategy. *Brain Res* 1134:1–11

Zhang L, Blomgren K, Kuhn HG, Cooper-Kuhn CM (2009) Effects of postnatal thyroid hormone deficiency on neurogenesis in the juvenile and adult rat. *Neurobiol Dis* 34:366–74

Zhang ZG, Zhang L, Jiang Q, Zhang R, Davies K, Powers C, Bruggen N, Chopp M (2000) VEGF enhances angiogenesis and promotes blood-brain barrier leakage in the ischemic brain. *J Clin Invest* 106:829–38